

Near-Infrared-Light Mediated Ratiometric Luminescent Sensor for Multimode Visualized Assays of Explosives

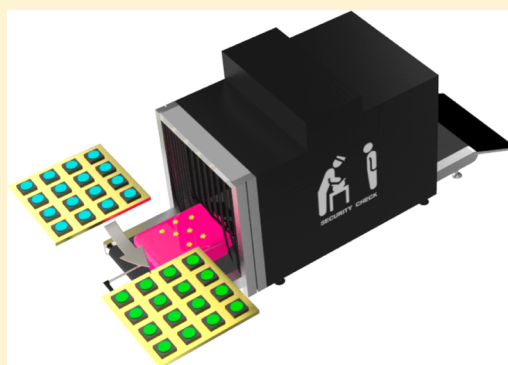
Xiaoxia Hu,^{†,§} Ting Wei,^{†,§} Jie Wang,[†] Zi-En Liu,[†] Xinyang Li,[†] Binhao Zhang,[†] Zhihao Li,[†] Lele Li,^{*,‡} and Quan Yuan^{*,†}

[†]Key Laboratory of Analytical Chemistry for Biology and Medicine (Ministry of Education), College of Chemistry and Molecular Sciences, Wuhan University, Wuhan, 430072, People's Republic of China

[‡]Department of Chemistry, University of Illinois at Urbana–Champaign, Urbana, Illinois 61801, United States

S Supporting Information

ABSTRACT: The development of a portable and easy-to-use device for the detection of explosives with high sensitivity and selectivity is in high demand for homeland security and public safety. In this study, we demonstrate miniaturized devices depending on the upconversion ratiometric luminescent probe for point-of-care (POC) assay of explosives with the naked-eye. When the PEI-coated upconversion nanoparticles (UCNPs) selectively bonded to 2,4,6-trinitrotoluene (TNT) explosives by the formation of Meisenheimer complex, the formed of UCNP–Meisenheimer complexes show turned visible multicolor upconversion luminescence (UCL) on account of TNT-modulating Förster resonance energy transfer process under near-infrared excitation. With UCL emission at 808 nm as internal standard and ratiometric UCL at 477 nm to that at 808 nm (I_{477}/I_{808}) as output signal, the probe can simultaneously meet the accuracy for TNT explosives quantitative analysis. In addition, this easy-to-use visual technique provides a powerful tool for convenient POC assay of rapid explosives identification.



A surge of suicide bombings and terrorist explosive attacks occurred around the world over the past several decades, according to press reports, which generally arise in confined spaces, such as subways, banks, and railway stations. The detection of potentially dangerous objects and items carried by suspicious people is quite necessary for preventing terrorist attacks. TNT, a high-powered explosive first synthesized in 1863,¹ has become a well-known explosive of choice for terrorists over the past decade.² Thus, detection of TNT explosives for counter-terrorism remains a high priority for a secure society in a wide variety of scenarios. Unfortunately, the detection methods for TNT used previously were commonly time-consuming and not portable, with the employment of complex instrumentation, such as gas chromatography or high-pressure liquid chromatography coupled with a mass spectrometer,³ surface-enhanced Raman spectroscopy,⁴ nuclear quadrupole resonance,⁵ and energy-dispersive X-ray diffraction.⁶ Since a handful of TNT explosives could remain adhered to the surfaces of packages with cautious hiding by terrorists,⁷ the development of a portable and easy-to-use device for the detection of explosives such as TNT with high sensitivity and selectivity at the security checkpoint is in high demand for homeland security and public safety.

Most recently, as an exciting new class of nanophosphors that convert near-infrared (NIR) excitation light into shorter-wavelength luminescence, lanthanide ion (Ln^{3+}) doped UCNPs have attracted great attention for sensing and imaging

applications.^{8–19} Since UCNPs can afford tunable multicolor upconversion luminescence (UCL) by controlling the Ln^{3+} dopants,¹⁰ they are an ideal choice for a ratiometric sensing technique. A ratiometric luminescence measurement, which permits signal rationing and employs ratiometric luminescence as the signal output, is promising to provide built-in correction for environment effects.¹¹ Furthermore, the photon upconversion can be produced under NIR excitation by a low-cost continuous-wave (CW) diode laser. Compared with a fluorescence-based technique, UCL-based measurement exhibits less autofluorescence and reduced light scattering, and thus can effectively avoid background interference.^{12–20} In particular, with extraordinarily high sensitivity and fast testing speed (<10 min), UCNPs are attractive for the development of POC devices.^{21,22}

Furthermore, the combination of the miniaturized analytical device with upconversion luminescence assay is likely to afford a promising tool for a POC assay with expected convenience, simplicity, and visibility, promoting the application of on-site detection of analytes.^{23,24} From a manufacturing point of view, we believe that the solid chips and patterned paper could be the attractive platforms available for developing assays. Particularly, the assay devices based on paper by immobilizing the Whatman

Received: August 28, 2014

Accepted: September 22, 2014

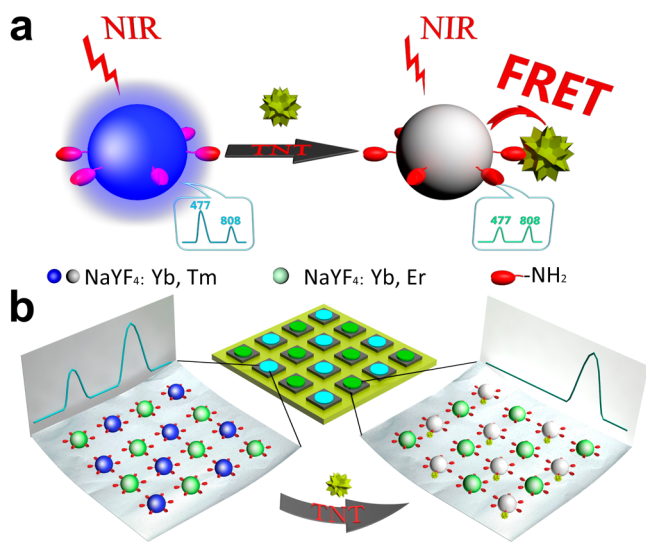
filter paper on the hydrophobic substrate to produce detection regions has recently been shown to be very attractive in the production of paper-based devices at low cost.²⁵ The upconversion luminescent sensor based device can lead to high sensitivity because the rather serious background fluorescence of additives and scattering light in the paper substrate can be perfectly avoided. Moreover, in comparison with conventional liquid detection methods, the detection region requires only a trace amount of analyte.

Herein, miniaturized devices depending on the upconversion ratiometric luminescent probe are demonstrated for the highly sensitive and selective detection of TNT explosives with the naked eye. These easy-to-use visual techniques provide a powerful tool for convenient POC assay of TNT by fixing nanoparticles onto the as-prepared substrates. These TNT-indicating devices exhibit multiple advantages, such as visualization, portability, and low cost. The easily performed technique contributes a lot to the development of on-site and rapid explosives identification devices, which holds great potential to exclude potentially dangerous events and thus provides a strong guarantee for public security.

RESULTS AND DISCUSSION

As shown in Scheme 1, the design principle is based on the TNT-modulated Förster resonance energy transfer (FRET)

Scheme 1. Working Principle for the Visual Detection of TNT based on a Ratiometric Luminescent Sensing Device



process between poly(ethylenimine) (PEI)-coated UCNP and Meisenheimer complex that is formed from primary amine group on the surface of UCNP and TNT target. PEI-coated UCNP are constructed with dual UCL bands at 477 and 808 nm, respectively. In the presence of TNT molecules, the blue UCL of the probe could be quenched due to the efficient FRET, while the unaffected NIR UCL of the probe at 808 nm serves as internal standard. In such a way, the ratiometric UCL at 477 nm to that at 808 nm (I_{477}/I_{808}) could be used as the output signal, leading to sensitive detection of TNT. Furthermore, we demonstrate the deposition of the ratiometric luminescent probes on the as-prepared substrate to create an integrated platform to visualize TNT with the naked eye for POC assay. As illustrated at the bottom of Scheme 1, the detection region of the miniature TNT-indicating device is

fixed with two kinds of UCNP, which emits multicolor UCL under NIR irradiation at 980 nm. When the detection region contacts with TNT, the blue UCL at 477 nm decreases dramatically through the FRET process, while the green UCL at 545 nm remains constant, which leads to the visual detection of TNT with the portable device.

PEI-coated NaYF₄: 18%Yb, 0.05% Tm nanoparticles were synthesized according to a previously reported protocol.²⁶ The transmission electron microscopy (TEM) image (Figure 1a) shows that the as-prepared nanoparticles exhibit uniform sizes and are nearly monodisperse, and the mean diameter of the particles was found to be 200 nm with a standard deviation of 18.7 nm. These as-prepared PEI modified UCNP possess excellent water solubility (inset image of Figure 1a). X-ray powder diffraction (XRD) pattern of UCNP (Figure 1b) shows that the diffraction lines are ascribed to the hexagonal structure of NaYF₄ with positions and intensities of the peaks in good agreement with the calculated values for hexagonal-NaYF₄ (JCPDS No. 16-0334). High-resolution TEM image (Supporting Information, SI, Figure S1) shows the highly ordered lattice array of the synthesized nanocrystal, which further confirms its highly crystalline structure. Compositional analysis of UCNP by energy-dispersive X-ray (EDX) measurement confirms that all the elements in the nanoparticles could be detected, including the codoped lanthanides Yb and Tm (SI Figure S2). The functionalization of PEI on the surface of UCNP was investigated by FTIR spectrophotometry. As shown in Figure 1c, the methylene asymmetric and symmetric C—H stretching (2960, 2850 cm⁻¹), amine N—H bending (1640 cm⁻¹), and amide bonds internal vibration (1380 cm⁻¹) are assigned to characteristic absorption peaks of PEI molecules, which have abundant electron-rich amino groups in the terminus for efficient reaction with electron-deficient TNT to form the Meisenheimer complex. The highly positive charge (33.7 mV) shown in the zeta potential measurement (SI Figure S3) further confirms the capping of amine terminated PEI on the surface of UCNP. The hydrodynamic diameters of UCNP were determined to be 240 nm with a standard deviation of 19.3 nm by dynamic light scattering (DLS), and the coefficient of variation is 9%, suggesting that PEI-coated UCNP were mostly monodispersed in water (SI Figure S4). Under NIR excitation at 980 nm, the PEI-coated NaYF₄: 18%Yb, 0.05% Tm nanoparticles show a strong blue emission band at 477 nm and a NIR emission band at 808 nm, which corresponds to the transition from ¹G₄ to ³H₆ and ³H₄ to ³H₆ of Tm³⁺, respectively (Figure 1d).^{26,27} The multiple UCL feature the utility of such materials for ratiometric luminescence detection under single 980 nm NIR excitation. Furthermore, the solution of these nanocrystals display bright blue luminescence (inset images of Figure 1d) under irradiation with a 980 nm CW laser, which indicates that the UCNP may be applied to visual detection of analytes.

The formation of Meisenheimer complex from TNT and primary amine group on the surface of UCNP is illustrated in Figure 2a. TNT is a strong electron-deficient aromatic ring due to three electron-withdrawing nitro groups, which can serve as electron acceptor.²⁸ While the organic amino groups can act as the electronic donors of nitroaromatic compounds through the electron transfer mechanism,^{29,30} a strong charge transfer interaction between the amino group of PEI and the nitro group could be obtained, thus leading to the formation of Meisenheimer complex. As shown in Figure 2b, color of the solution containing UCNP-based probes dramatically changes

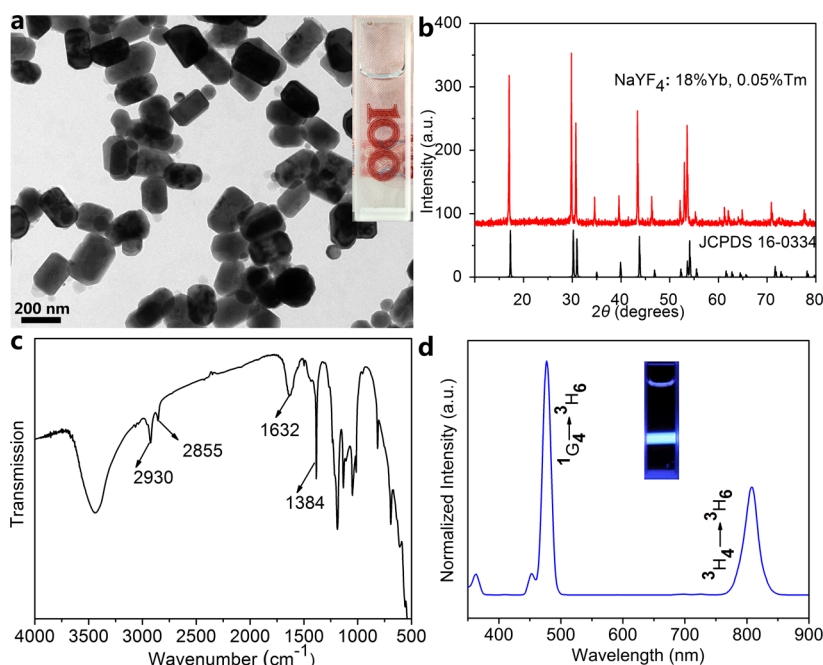


Figure 1. (a) TEM image of PEI-coated NaYF₄: 18%Yb, 0.05% Tm UCNPs. Insert: photograph of PEI-coated UCNPs dispersed in water. (b) XRD patterns of PEI-coated NaYF₄: 18%Yb, 0.05% Tm. (c) FTIR absorption spectrum of PEI-coated UCNPs. (d) Upconversion luminescence spectrum of PEI-coated NaYF₄: 18%Yb, 0.05% Tm. Insert: corresponding luminescence photograph of PEI-coated UCNPs under 980 nm laser illumination.

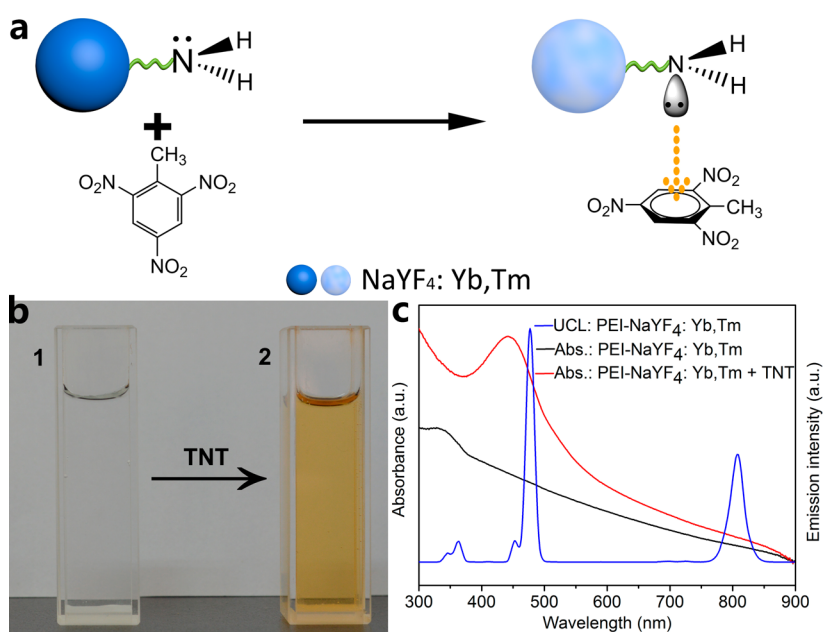


Figure 2. (a) Schematic representation of the interaction between electron-rich amino group on the surface of UCNPs and electron-deficient aromatic ring of TNT through charge-transfer mechanism to form the Meisenheimer complex. (b) The photographs of PEI-coated UCNPs before (left) and after (right) addition of TNT under natural light. (c) The absorption spectra of PEI-coated NaYF₄: Yb, Tm UCNPs before and after addition of TNT plotted together with the UCL emission spectrum of PEI-coated NaYF₄: Yb, Tm UCNPs in solution.

from colorless into orange with the addition of TNT, which matches the absorption characteristic of the Meisenheimer complexes. The corresponding UV–vis spectrum of the complex solution shows a strong absorption band at 445 nm (Figure 2c), which overlaps well with the blue UCL emission of the UCNPs-based probe and results in the potential FRET process from the excited UCNPs to the complexes.

We further investigate the UCL response of the UCNPs-based probe to TNT. Under irradiation with a 980 nm CW

laser, the probe displays multiple emission peaks, in which two well-resolved emission peaks at 477 and 808 nm are suitable to achieve “self-calibrating” ratiometric detection. In the presence of TNT molecules, the UCL at 477 nm decreases gradually while the NIR UCL at 808 nm stays unaffected (Figure 3), and the ratio I_{477}/I_{808} is found to be linear within the TNT represents ratio I_{477}/I_{808} with a correlation coefficient of 0.9905 (SI Figure S5). Thus, the luminescent probe used here could be employed for ratiometric sensing of TNT.

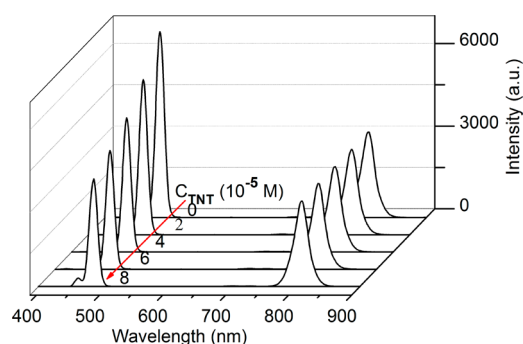


Figure 3. Dependence of the ratiometric UCL spectra of the NaYF₄: Yb, Tm UCNPs upon exposure to different amount of TNT.

We test whether the UCNPs-based probe could be used for TNT detection on solid chips since microchip methods require only a trace amount of analyte due to its highly integrated substrate.^{31–33} As shown in Figure 4a, nanoprobe were assembled into the microwell array of the designed microchip through an evaporation-induced casting method. The brightness of UCL spots is gradually weakened with the increase of TNT concentration from 1×10^{-9} to 10^{-5} M under NIR excitation (Figure 4b). The luminescence from the microchip is visible even with the naked eye due to the intensive emission of NaYF₄: Yb, Tm nanoparticles and it can be captured by a standard digital single-lens reflex camera equipped with a macro lens.

For the ratiometric visual detection of TNT explosives, PAA-coated NaYF₄: 20%Yb, 2%Er UCNPs exhibiting green UCL under 980 nm CW laser illumination has been further synthesized. The TEM images of the NaYF₄: 20%Yb, 2%Er nanoparticles show that the nanoparticles have well-defined hexagonal shapes, and the mean diameter was found to be 246 nm with a standard deviation of 20.9 nm from a detailed particle size analysis of 500 particles from several low-resolution TEM micrographs (Figure 5a and SI Figure S6). To convert hydrophobic oleic acid (OA)-coated NaYF₄: Yb, Er UCNPs into hydrophilic ones, poly(acrylic acid) (PAA) coating methods by a modified ligand exchange procedure was used here. After exchanging with OA, the resultant PAA-coated UCNPs possess good dispersibility in aqueous solution (insert image of Figure 5a). Additionally, this functionalized UCNPs can not react with TNT analyte, thus avoiding potential interruption and leading to high sensitivity. Under excitation of CW laser at 980 nm, Er-doped UCNPs show green and red

emission bands at 545 and 658 nm, which can be attributed to the transition from $^4S_{3/2}$ to $^4I_{15/2}$ and $^4F_{9/2}$ to $^4I_{15/2}$ of Er³⁺ (Figure 5b). By mixing PEI-coated NaYF₄: 18%Yb, 0.05%Tm and PAA-coated NaYF₄: 20%Yb, 2%Er nanoparticles at a certain ratio (mol/mol, 3:1), the resultant hybrid ratiometric luminescent probe exhibit multicolor UCL, containing blue, green, and red emission band at 477, 545, and 658 nm (Figure 5c), and the solution of these hybrid probes finally display bright bluish green luminescence under NIR irradiation (inset image of Figure 5c).

To achieve the visualized identification of trace TNT in a portable way, a solid microchip has been fabricated, which has 10×10 microarrays of ratiometric luminescent probe (PEI-coated NaYF₄: 18%Yb, 0.05%Tm and PAA-coated NaYF₄: 20%Yb, 2%Er) spots within 0.49 cm² (Figure 6a). The luminescent dot arrays is highly regular and exhibit bluish green luminescence under 980 nm laser excitation (Figure 6b) and then the color of luminescent dots instantly change into green in the presence of 20 ng TNT since the part of blue UCL can be quenched in the presence of TNT (Figure 6c).

In order to demonstrate an easy-to-use and inexpensive device, a novel strategy has been developed by immobilizing the hybrid ratiometric luminescent probes onto the paper-based platform. As illustrated in Figure 7a, the underlays are first bonded to the adhesive backing to form a test array. Then, the resultant patterned paper is constructed by immobilizing the circular Whatman filter paper on the underlay to form the test zone. A zone diameter of 5 mm with a spacing of 3 mm between zones is selected to keep the use of reagents as low as possible. The TNT-indicating paper is finally developed by assembling the probes on the test zone of the as-prepared paper and the test zone display obvious color change upon exposure to TNT under NIR excitation (Figure 7b). This assembly approach is simple and convenient, which meets the requirements of batch production and low cost. The photograph of the as-prepared paper-based device is shown in Figure 7c, and it emits bluish green luminescence under NIR excitation (Figure 7d). In the presence of trace TNT residues (20 ng), the color of the test zone turns into orange (Figure 7e) and the luminescence of the test zone instantly changes into green within 3 s (Figure 7f). These results indicate that the paper-based TNT-indicating device is highly desirable to demonstrate the instant, convenient, and visualized POC detection of TNT carried by terrorists.

The ratiometric nanoprobe also exhibits high selectivity for target TNT over some other nitroaromatics explosives such as

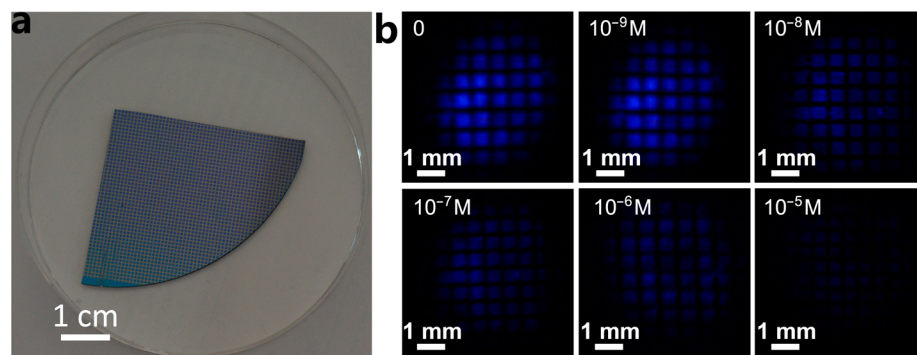


Figure 4. (a) The image of silicon wafer with microwell array for the device fabrication. (b) Luminescence images of the UCNPs based microarrays sensing platform in the presence of different amount of TNT.

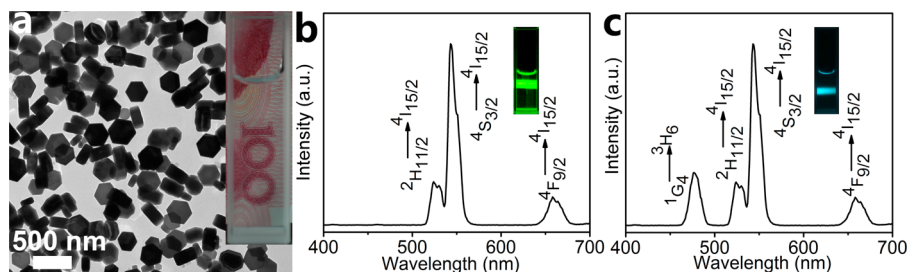


Figure 5. (a) TEM image of PAA-coated UCNPs. Insert: photograph of PAA-coated UCNPs dispersed in water. (b) Upconversion luminescence spectrum of PAA-coated NaYF₄: 20%Yb, 2%Er. Insert: corresponding luminescence photograph of PAA-coated UCNPs under 980 nm laser illumination. (c) Upconversion luminescence spectrum of hybrid ratiometric luminescent probe. Insert: corresponding luminescence photograph of hybrid probe under 980 nm laser illumination.

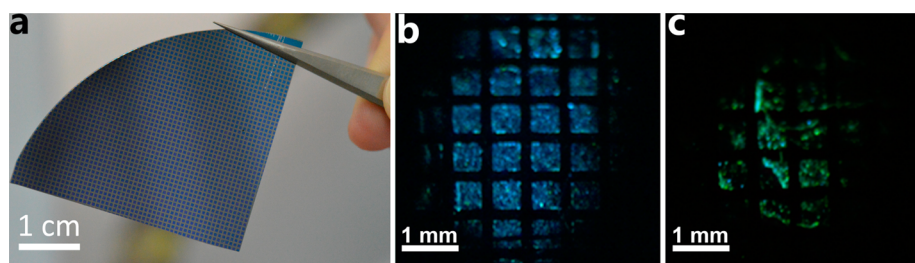


Figure 6. (a) Photograph of the silicon wafer with microarrays. Luminescence photographs of the hybrid ratiometric luminescent probe based microarrays in absence (b) and presence (c) of trace TNT.

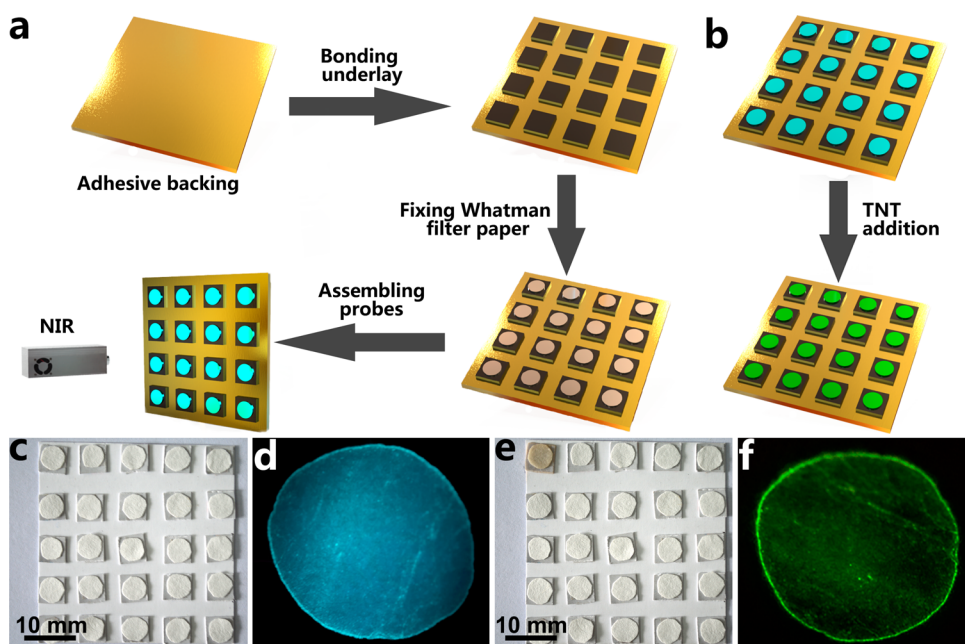


Figure 7. (a) Schematic illustration of the ratiometric visual identification of TNT by assembling the hybrid ratiometric luminescent probe onto a paper substrate. (b) Schematic diagram of TNT explosives detection based on the as-prepared TNT-indicating paper. The images of TNT-indicating paper under nature light (c) and under CW 980 nm laser illumination (d). The photographs of TNT-indicating paper with the addition of trace TNT under nature light (e) and under excitation with a CW 980 nm laser (f).

2,4-dinitrotoluene (DNT) and nitrobenzene (NB). The evolution of UV–vis absorption (Figure 8a) of the nanoprobe in the presence of DNT or NB do not show any absorption band around 477 nm, and no change of system color has been observed (Figure 8b). Since DNT and NB are much weaker electronic acceptors compared with TNT, they are not likely to form the effective Meisenheimer complex with amine groups on the surface of UCNPs. It should be mentioned that I_0 and I are, respectively, the luminescence intensity of the nano-

particles suspension before and after the addition of nitroaromatics (40 μM). As shown in Figure 8c, 40 μM of nitrobenzene (NB) and 2,4-dinitrotoluene (DNT) contributed little changes in luminescence ratio of I/I_0 . However, TNT caused a dramatic decrease in the luminescence intensity (the ratio of I/I_0 is far below 1.0). Meanwhile, compared with TNT, DNT, or NB induces less change of the luminescence intensity in solution (Figure 8d), suggesting the high selectivity of the sensing probe. The high selectivity of the ratiometric

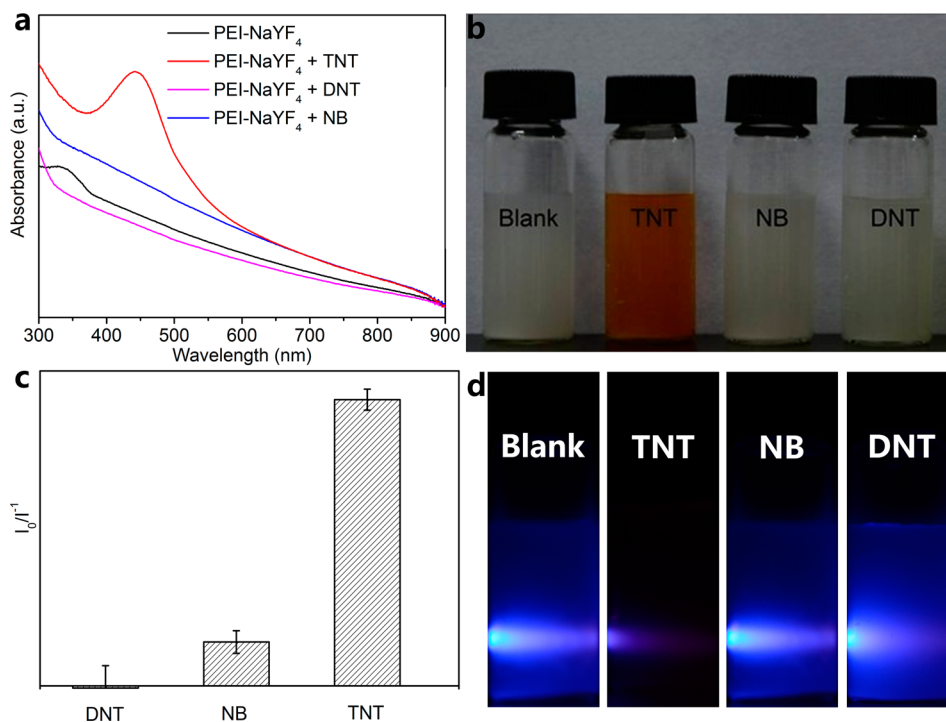


Figure 8. (a) Evolution of UV–vis absorption spectra with the addition of DNT, NB, and TNT into 2 mL solution containing 1 mg mL⁻¹ PEI-coated UCNPs, respectively. The final concentration of nitroaromatics is 40 μM. (b) Photographs of PEI-coated UCNPs for specific identification of TNT from other similar nitroaromatics under natural light. Demonstration of selectivity of PEI-coated UCNPs for TNT over other nitroaromatic compounds (c), and the corresponding luminescence photographs under 980 nm NIR irradiation (d).

nanoprobe can greatly reduce the potential of false positives and can evaluate the threat by the identification of the explosive structures.

CONCLUSIONS

In summary, a novel paper-based ratiometric luminescent device depending on multicolor UCNPs has been successfully developed for the visualization of TNT explosives. TNT molecules can selectively bind to PEI-coated UCNPs to form the Meisenheimer complex, thus leading to the FRET with the multicolor UCNPs as energy donor and the formed complex as energy acceptor. This method shows high sensitivity and selectivity for TNT explosives with the naked eye. Furthermore, a paper-based TNT-indicating device has been innovated to visualize TNT for POC assay through the UCL color change of probe. This technique built upon upconversion ratiometric luminescent probe reported herein possesses great potential for getting rid of potential risks in time at the safety inspecting system, and thus provides great assurance for public security. On the basis of this strategy, we further anticipate that this method will find wide-ranging applications in environmental monitoring, biological processes imaging, and personalized healthcare.

EXPERIMENTAL SECTION

Synthesis of PEI-coated NaYF₄: Yb, Tm, UCNPs. Water-soluble PEI-coated UCNPs were prepared by a one-pot hydrothermal method.²⁶ In a typical synthesis of PEI-coated NaYF₄: 18%Yb, 0.05% Tm nanoparticles, 10 mL of NaCl, 10 mL of LnCl₃ (Y/Yb/Tm = 81.95:18:0.05 in mol), 20 mL of PEI stock solutions and 60 mL of ethanol were added to a 200 mL flask. Thereafter, 12 mmol of NH₄F (with F⁻/Ln³⁺ = 6, mol/mol ratio) was added to the above solution with vigorous stirring. The mixture was then transferred to a Teflon autoclave and heated to 200 °C for 24 h. After cooling to room

temperature, the PEI-coated NaYF₄: Yb, Tm nanoparticles were obtained by centrifugation, washed with ethanol and water (v/v, 1:1) for three times, and dried under vacuum before use.

Synthesis of PAA-Coated NaYF₄: Yb, Er UCNPs. Hexagonal phase OA-coated NaYF₄: 20% Yb, 2% Er nanoparticles were first synthesized using a previously reported protocol.³⁴ 1 mmol of CF₃COONa and a suitable proportion of Y(CF₃COO)₃, Yb(CF₃COO)₃, and Er(CF₃COO)₃ were added to a mixture of OA (20 mmol) and ODE (20 mmol) in a 100 mL three-necked flask. Next, the slurry was heated to 120 °C for 0.5 h with vigorous stirring under vacuum. The resulting solution was then heated to 340 °C at a heating rate of 20 °C min⁻¹, and was maintained at this temperature for 0.5 h under an Ar atmosphere. After cooling to room temperature, the obtained OA-coated UCNPs were washed with ethanol and cyclohexane (v/v, 1:1) for three times and recovered by centrifugation. After that, 30 mL of DEG and 300 mg of PAA-1800 were added to a 100 mL three-necked flask. The mixture was heated to 110 °C to form a pellucid solution under vacuum, then a mixed solution of toluene and chloroform containing 100 mg of the as-prepared OA-coated UCNPs was slowly added into the flask and reacted for 1 h under argon protection. The solution was then heated to 240 °C and the temperature maintained for 1.5 h. After cooling down to room temperature, ethanol was added to yield the PAA-coated UCNPs precipitate. The PAA-coated UCNPs nanoparticles were washed three times with ethanol and water (v/v, 1:1) and recovered by centrifugation.³⁵ Finally, the obtained PAA-coated UCNPs were dispersed in 100 mL of water.

Ratiometric Luminescent Response of PEI-Coated NaYF₄ Nanoparticles to Nitroaromatics. In brief, 100 μL of ratiometric probe solution was added to a tube, followed by the addition of various amounts of TNT. Then, the mixed solution was diluted to 2.0 mL with ultrapure water. The final concentration of ratiometric probe solution for the measurements of luminescence quenching was 1 mg mL⁻¹. Finally, the mixture was transferred to a spectrophotometer quartz cuvette. The ratiometric luminescent response to nitroaromatics were collected on a Hitachi F-4600 luminescence spectrometer under irradiation with a 980 nm CW laser.

Probe-Assembled Chips for the Detection of TNT Explosives. The microwell array was fabricated by using a standard photolithographic technique. AZ5214 photoresist was first coated onto the surface of a silicon wafer. After exposure to UV light under a photomask, the pattern of the dot array with 500 μm in side length was formed by immersing the silicon wafer into the developing solution. The nanoprobe arrays were assembled into the microwell array of the silicon wafer through an evaporation-induced casting method. By removing the remaining photoresist with acetone, the microwells spontaneously filled up with the UCNPs. The luminescence sensitivity to the various analytes was tested by dropping trace amounts of analyte solution onto the silicon chips, and luminescent images of the dot arrays were then taken by using a standard digital single-lens reflex camera equipped with a macro lens.

Paper-Based Ratiometric Luminescent Device for Visual Detection of TNT Explosives. The ratiometric probe solution for visual detection was prepared by hybridizing PEI-coated NaYF_4 : Yb, Tm nanoparticles and PAA-coated NaYF_4 : Yb, Er nanoparticles with a volume ratio of 3:1. A piece of cardboard was first prepared as an adhesive backing. Then, the underlays were bonded to the adhesive backing to form a 5×5 array. The resultant patterned paper was last constructed by immobilizing the circular Whatman filter paper (test zone) on the underlay. The diameter of the detection region was 5 mm, requiring 5 μL of solution containing ratiometric luminescent probe. The probes were assembled to the test zone of the as-prepared paper and dried at 50 $^\circ\text{C}$ for 10 min. This TNT-indicating paper displayed strong blue-green luminescence under irradiation with a 980 nm CW laser. To demonstrate its application as a luminescent paper sensor for TNT detection, 9 μL of the known concentration (1×10^{-5} M) of analytes was exposed to the test zone of the TNT-indicating paper. Thereafter, the luminescence color responses of the test zone was observed under NIR irradiation with a 980 nm CW laser (0.5 W) and the luminescent photos were taken by a digital camera.

ASSOCIATED CONTENT

Supporting Information

Chemicals; instruments; HRTEM image PEI-coated NaYF_4 : 18%Yb, 0.05% Tm UCNPs (Figure S1); EDX analysis of PEI-coated NaYF_4 : 18%Yb, 0.05%Tm UCNPs (Figure S2); Zeta potential of PEI-coated NaYF_4 : 18%Yb, 0.05%Tm UCNPs (Figure S3); dynamic light scattering pattern of PEI-coated NaYF_4 : 18%Yb, 0.05% Tm UCNPs (Figure S4); changes in luminescence intensity of the ratiometric probe solution at 477 nm versus that at 808 nm upon the addition of TNT (Figure S5); (a) TEM image of OA-coated NaYF_4 : 20%Yb, 2%Er UCNPs, (b) HRTEM images of the OA-coated UCNPs (Figure S6); XRD analysis of NaYF_4 : 20%Yb, 2%Er UCNPs (Figure S7); EDX analysis of PAA-coated NaYF_4 : 20%Yb, 2%Er UCNPs (Figure S8); Zeta potential of PAA-coated NaYF_4 : 20% Yb, 2%Er UCNPs (Figure S9); and the luminescence images of ratiometric luminescent probe solution before (a) and after (b) TNT addition under irradiation with a 980 nm CW laser (Figure S10). This material is available free of charge via the Internet at <http://pubs.acs.org/>.

AUTHOR INFORMATION

Corresponding Authors

*E-mail: yuanquan@whu.edu.cn.

*E-mail: leleli2008@gmail.com.

Author Contributions

[§]These authors contributed equally to this work.

Notes

The authors declare no competing financial interest.

ACKNOWLEDGMENTS

This work was supported by the National Natural Science Foundation of China (21201133, 51272186) and the Fundamental Research Funds for the Central Universities. Q.Y. thanks the large-scale instrument and equipment sharing foundation of Wuhan University.

REFERENCES

- (1) Yinon, J. *Forensic and Environmental Detection of Explosives*; John Wiley & Sons Ltd: Chichester, 1999.
- (2) Singh, S. J. *Hazard. Mater.* **2007**, *144*, 15–28.
- (3) Hakansson, K.; Coorey, R. V.; Zubarev, R. A.; Talrose, V. L.; Hakansson, P. J. *Mass Spectrom.* **2000**, *35*, 337–346.
- (4) Sylvia, J. M.; Janni, J. A.; Klein, J. D.; Spencer, K. M. *Anal. Chem.* **2000**, *72*, 5834–5840.
- (5) Anferov, V. P.; Mozjoukhine, G. V.; Fisher, R. *Rev. Sci. Instrum.* **2000**, *71*, 1656–1659.
- (6) Luggar, R. D.; Farquharson, M. J.; Horrocks, J. A.; Lacey, R. J. *X-Ray Spectrom.* **1998**, *27*, 87–94.
- (7) Zhang, W. X. *J. Nanopart. Res.* **2003**, *5*, 323–332.
- (8) Wang, G. F.; Peng, Q.; Li, Y. D. *Acc. Chem. Res.* **2011**, *44*, 322–332.
- (9) Dai, Y. L.; Xiao, H. H.; Liu, J. H.; Yuan, Q. H.; Ma, P. A.; Yang, D. M.; Li, C. X.; Cheng, Z. Y.; Hou, Z. Y.; Yang, P. P.; Lin, J. *J. Am. Chem. Soc.* **2013**, *135*, 18920–18929.
- (10) Yi, G. S.; Chow, G. M. *J. Mater. Chem.* **2005**, *15*, 4460–4464.
- (11) Liu, J. L.; Liu, Y.; Liu, Q.; Li, C. Y.; Sun, L. N.; Li, F. Y. *J. Am. Chem. Soc.* **2011**, *133*, 15276–15279.
- (12) Gai, S. L.; Li, C. X.; Yang, P. P.; Lin, J. *Chem. Rev.* **2014**, *114*, 2343–2389.
- (13) Dai, Y. L.; Ma, P. A.; Cheng, Z. Y.; Kang, X. J.; Zhang, X.; Hou, Z. Y.; Li, C. X.; Yang, D. M.; Zhai, X. F.; Lin, J. *ACS Nano* **2012**, *6*, 3327–3338.
- (14) Wei, W.; He, T. C.; Teng, X.; Wu, S. X.; Ma, L.; Zhang, H.; Ma, J.; Yang, Y. H.; Chen, H. Y.; Han, Y.; Sun, H. D.; Huang, L. *Small* **2012**, *8*, 2271–2276.
- (15) Li, L. L.; Zhang, R. B.; Yin, L. L.; Zheng, K. Z.; Qin, W. P.; Selvin, P. R.; Lu, Y. *Angew. Chem., Int. Ed.* **2012**, *51*, 6121–6125.
- (16) Yang, Y. M.; Shao, Q.; Deng, R. R.; Wang, C.; Teng, X.; Cheng, K.; Huang, Z.; Cheng, L.; Liu, Z.; Liu, X. G.; Xing, B. G. *Angew. Chem., Int. Ed.* **2012**, *51*, 3125–3129.
- (17) Li, C. X.; Lin, J. *J. Mater. Chem.* **2010**, *20*, 6831–6847.
- (18) Tu, D. T.; Liu, L. Q.; Ju, Q.; Liu, Y. S.; Zhu, H. M.; Li, R. F.; Chen, X. Y. *Angew. Chem., Int. Ed.* **2011**, *50*, 6306–6310.
- (19) Yuan, Q.; Wu, Y.; Wang, J.; Lu, D. Q.; Zhao, Z. L.; Liu, T.; Zhang, X. B.; Tan, W. H. *Angew. Chem., Int. Ed.* **2013**, *52*, 13965–13969.
- (20) Tang, L. H.; Chun, I. S.; Wang, Z. D.; Li, J. H.; Li, X. L.; Lu, Y. *Anal. Chem.* **2013**, *85*, 9522–9527.
- (21) Lin, M.; Zhao, Y.; Wang, S. Q.; Liu, M.; Duan, Z. F.; Chen, Y. M.; Li, F.; Xu, F.; Lu, T. *J. Biotechnol. Adv.* **2012**, *30*, 1551–1561.
- (22) Corstjens, P.; Zuiderwijk, M.; Brink, A.; Li, S.; Feindt, H.; Niedbala, R. S.; Tanke, H. *Clin. Chem.* **2001**, *47*, 1885–1893.
- (23) Kaushik, A.; Vasudev, A.; Arya, S. K.; Pasha, S. K.; Bhansali, S. *Biosens. Bioelectron.* **2014**, *53*, 499–512.
- (24) Zhou, F.; Noor, M. O.; Krull, U. *J. Anal. Chem.* **2014**, *86*, 2719–2726.
- (25) Liana, D. D.; Raguse, B.; Gooding, J. J.; Chow, E. *Sensors* **2012**, *12*, 11505–11526.
- (26) Wang, F.; Chatterjee, D. K.; Li, Z. Q.; Zhang, Y.; Fan, X. P.; Wang, M. Q. *Nanotechnology* **2006**, *17*, 5786–5796.
- (27) Auzel, F. *Chem. Rev.* **2004**, *104*, 139–173.
- (28) Bernasconi, C. F. *J. Org. Chem.* **1971**, *36*, 1671–1679.
- (29) Gao, D. M.; Wang, Z. Y.; Liu, B. H.; Ni, L.; Wu, M. H.; Zhang, Z. P. *Anal. Chem.* **2008**, *80*, 8545–8553.
- (30) Jiang, Y.; Zhao, H.; Zhu, N. N.; Lin, Y. Q.; Yu, P.; Mao, L. Q. *Angew. Chem., Int. Ed.* **2008**, *47*, 8601–8604.
- (31) Chen, G.; Wang, J. *Analyst* **2004**, *129*, 507–511.

(32) Hu, M.; Yan, J.; He, Y.; Lu, H. T.; Weng, L. X.; Song, S. P.; Fan, C. H.; Wang, L. H. *ACS Nano* **2010**, *4*, 488–494.

(33) Liu, Y. Y.; Sun, Y.; Sun, K.; Song, L. S.; Jiang, X. Y. *J. Mater. Chem.* **2010**, *20*, 7305–7311.

(34) Mai, H. X.; Zhang, Y. W.; Si, R.; Yan, Z. G.; Sun, L. D.; You, L. P.; Yan, C. H. *J. Am. Chem. Soc.* **2006**, *128*, 6426–6436.

(35) Xiong, L. Q.; Yang, T. S.; Yang, Y.; Xu, C. J.; Li, F. Y. *Biomaterials* **2010**, *31*, 7078–7085.